RESEARCH ARTICLE
Therapeutics and Prevention

Mapping the Role of AcrAB-TolC Efflux Pumps in the Evolution of Antibiotic Resistance Reveals Near-MIC Treatments Facilitate Resistance Acquisition

Ariel M. Langevin,[a,b] Imane El Meouche,[a,b]* Mary J. Dunlop[a,b]

[a]Department of Biomedical Engineering, Boston University, Boston, Massachusetts, USA
[b]Biological Design Center, Boston, Massachusetts, USA

ABSTRACT Antibiotic resistance has become a major public health concern as bacteria evolve to evade drugs, leading to recurring infections and a decrease in antibiotic efficacy. Systematic efforts have revealed mechanisms involved in resistance. Yet, in many cases, how these specific mechanisms accelerate or slow the evolution of resistance remains unclear. Here, we conducted a systematic study of the impact of the AcrAB-TolC efflux pump on the evolution of antibiotic resistance. We mapped how population growth rate and resistance change over time as a function of both the antibiotic concentration and the parent strain's genetic background. We compared the wild-type strain to a strain overexpressing AcrAB-TolC pumps and a strain lacking functional pumps. In all cases, resistance emerged when cultures were treated with chloramphenicol concentrations near the MIC of their respective parent strain. The genetic background of the parent strain also influenced resistance acquisition. The wild-type strain evolved resistance within 24 h through mutations in the *acrAB* operon and its associated regulators. Meanwhile, the strain overexpressing AcrAB-TolC evolved resistance more slowly than the wild-type strain; this strain achieved resistance in part through point mutations in *acrB* and the *acrAB* promoter. Surprisingly, the strain without functional AcrAB-TolC efflux pumps still gained resistance, which it achieved through upregulation of redundant efflux pumps. Overall, our results suggest that treatment conditions just above the MIC pose the largest risk for the evolution of resistance and that AcrAB-TolC efflux pumps impact the pathway by which chloramphenicol resistance is achieved.

IMPORTANCE Combatting the rise of antibiotic resistance is a significant challenge. Efflux pumps are an important contributor to drug resistance; they exist across many cell types and can export numerous classes of antibiotics. Cells can regulate pump expression to maintain low intracellular drug concentrations. Here, we explored how resistance emerged depending on the antibiotic concentration, as well as the presence of efflux pumps and their regulators. We found that treatments near antibiotic concentrations that inhibit the parent strain's growth were most likely to promote resistance. While wild-type, pump overexpression, and pump knockout strains were all able to evolve resistance, they differed in the absolute level of resistance evolved, the speed at which they achieved resistance, and the genetic pathways involved. These results indicate that specific treatment regimens may be especially problematic for the evolution of resistance and that the strain background can influence how resistance is achieved.

KEYWORDS AcrAB-TolC, antibiotic resistance, efflux pump

Despite the new wave of antibiotic discovery (1–5), bacteria continue to acquire resistance shortly after the introduction of new drugs for medicinal and industrial applications (6, 7). This is due in large part to the overuse of antibiotics, which results

Citation Langevin AM, El Meouche I, Dunlop MJ. 2020. Mapping the role of AcrAB-TolC efflux pumps in the evolution of antibiotic resistance reveals near-MIC treatments facilitate resistance acquisition. mSphere 5:e01056-20. https://doi.org/10.1128/mSphere.01056-20.

Editor Ana Cristina Gales, Escola Paulista de Medicina/Universidade Federal de São Paulo

Address correspondence to Mary J. Dunlop, mjdunlop@bu.edu.

* Present address: Imane El Meouche, Université de Paris, IAME, UMR1137, INSERM, Paris, France.

Received 17 October 2020
Accepted 29 November 2020
Published 16 December 2020

in pressures that drive resistance (8). With limited novel antibiotics and numerous futile antibiotics, doctors and scientists alike are presented with the challenge of how to best treat infections while keeping the evolution of resistance in check.

Adaptive evolution studies have begun exploring how certain antibiotic pressures influence the evolution of resistance. For instance, studies using a "morbidostat"—a continuous culture device that dynamically adjusts antibiotic concentrations to inhibitory levels—have found numerous targets that can be readily mutated to promote resistance (9–11), as well as identifying how drug switching can limit the evolution of resistance (12). While these studies have provided pivotal insights for this field, the morbidostat design causes antibiotic concentrations to rise to levels that exceed clinically relevant concentrations due to toxicity for patients (13). In recognition of the drug concentration-dependent nature of evolution, researchers have begun to explore bacterial evolution under treatment conditions with lower antibiotic concentrations as well. Wistrand-Yuen et al. found that bacteria grown at subinhibitory drug concentrations were still able to achieve high levels of resistance (14–16). Notably, the study identified that the same antibiotic produced unique evolutionary pathways when cells were treated with subinhibitory concentrations as opposed to inhibitory concentrations (14).

One limitation of current studies within the field is that they can be difficult to compare due to variations in experimental parameters, such as species, antibiotics, or other experimental conditions (17). Given the unique evolutionary pathways at different antibiotic concentrations, systematic mapping of these evolutionary landscapes could provide an improved understanding of which conditions pose the highest risk by allowing direct comparisons between different antibiotic concentrations. For instance, Jahn et al. demonstrated that variations in treatment dynamics can significantly alter evolved resistance for some antibiotics, such as tetracycline, but not others, such as amikacin and piperacillin (18). Other evolution experiments that were systematically conducted using a range of concentrations for β-lactams (19) and erythromycin (20) have highlighted the concentration-dependent adaptability of *Escherichia coli*.

There are many mechanisms by which antibiotic resistance can be achieved, including enzymatic inactivation, alteration of antibiotic binding sites, and increased efflux or reduced influx of antibiotics (21, 22). Efflux pumps are omnipresent in prokaryotic and eukaryotic cells alike and are an important contributor to multidrug resistance (23). AcrAB-TolC in *E. coli* is a canonical example of a multidrug efflux pump, providing broad-spectrum resistance and raising the MIC of at least nine different classes of antibiotics (24). The pump is composed of three types of proteins: the outer membrane channel protein, TolC; the periplasmic linker protein, AcrA; and the inner membrane protein responsible for substrate recognition and export, AcrB (23). Using the proton motive force, AcrB actively exports antibiotics from the cell (23, 25). The presence of AcrAB-TolC efflux pumps can increase a strain's MIC from ~2-fold to ~10-fold, depending on the antibiotic (26–28). Furthermore, genes associated with these multidrug-resistant efflux pumps, including their local and global regulators, are common targets for mutation as strains evolve high levels of drug resistance (15, 29–32).

Recent studies have indicated that in addition to providing modest increases in the MIC due to drug export, pumps can also impact mutation rate and evolvability of strains, which may ultimately be more important for the acquisition of high levels of drug resistance. For example, Singh et al. found that mutants overexpressing *acrAB* emerged first, and afterwards these mutants could evolve high levels of quinolone resistance (33). In addition, heterogeneity in efflux pump expression can predispose subsets of bacterial populations with elevated *acrAB* expression to mutation even prior to antibiotic treatment (34). Deletion of genes associated with efflux pumps, such as *tolC*, can also reduce evolvability under antibiotic exposure (35). Furthermore, a recent study in *Staphylococcus aureus* found that higher NorA pump levels increased evolvability and that addition of a pump inhibitor could prevent resistance evolution (36).

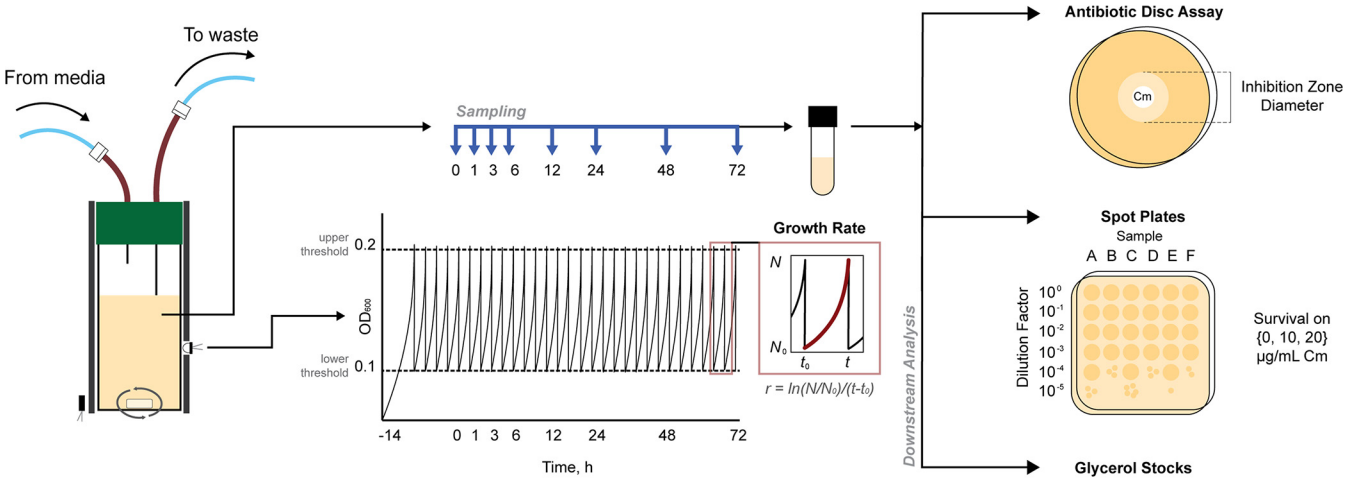

FIG 1 Evolution experiment schematic. We used the eVOLVER, a modular turbidostat, as an evolutionary platform to measure and record cell density by measuring absorbance at 600 nm (OD_{600}). We calculated the growth rate after each dilution event and collected samples at defined time points ($t = 0$, 1, 3, 6, 12, 24, 48, and 72 h). We performed antibiotic disc assays and spot plate assays for all samples.

These studies provoke the question of how AcrAB-TolC efflux pumps impact the evolution of drug resistance.

Our overall goal in this study was to identify how strains with different AcrAB-TolC genotypes evolve antibiotic resistance over time under a range of chloramphenicol concentrations. Chloramphenicol is both a well-validated substrate of AcrAB-TolC and can serve as a last resort antibiotic in multidrug-resistant infections, as most clinical isolates are still susceptible to this drug (37, 38). To identify how AcrAB-TolC impacts the evolution of resistance, we used a turbidostat as an evolutionary platform (39) and measured changes in fitness and resistance. We evolved three strains with different levels of AcrAB-TolC: a wild-type (WT) strain with the native regulatory network controlling AcrAB-TolC expression; a strain that lacks the local regulator AcrR ($AcrAB^+$), which results in a 1.5- to 6-fold increase in expression of the pumps (40–42); and a strain lacking functional AcrAB-TolC efflux pumps (Δ*acrB*). We allowed the cultures to grow and evolve for 72 h in continuous culture while continuously recording growth rates. We periodically sampled the cultures and assessed the population's resistance. We then charted the evolutionary landscapes for each of the three strains under different chloramphenicol concentrations to identify which circumstances gave rise to resistance.

RESULTS

In order to systematically evaluate the evolutionary landscape of efflux pump-mediated antibiotic resistance, we used the eVOLVER, a modular turbidostat capable of growing independent cultures in parallel (39). This platform allowed us to track a culture's fitness by measuring growth rate continuously over multiday experiments. In addition to this, we collected samples at selected intervals and, with these samples, performed antibiotic disc diffusion assays to assess the population's resistance and spot assays to quantify the presence of high-resistance isolates within the population (Fig. 1).

We mapped growth rates over time for cultures subjected to a range of chloramphenicol treatment concentrations (Fig. 2A; see Fig. S1 in the supplemental material). To compare across strains, we defined MIC^0_{parent} as the MIC of the parent strain (MIC^0_{WT} = 2 μg/ml, MIC^0_{AcrAB+} = 2 μg/ml, and $MIC^0_{\Delta acrB}$ = 0.5 μg/ml). We found similar values for MIC^0_{WT} and MIC^0_{AcrAB+} (see Fig. S2 in the supplemental material), which may be due to induction of efflux pump expression in the WT strain in the presence of chloramphenicol. Prior studies have shown that the presence of stress can increase pump expression by 4-fold (40, 43), which is comparable to the impact of deleting *acrR* (40–42). We found that

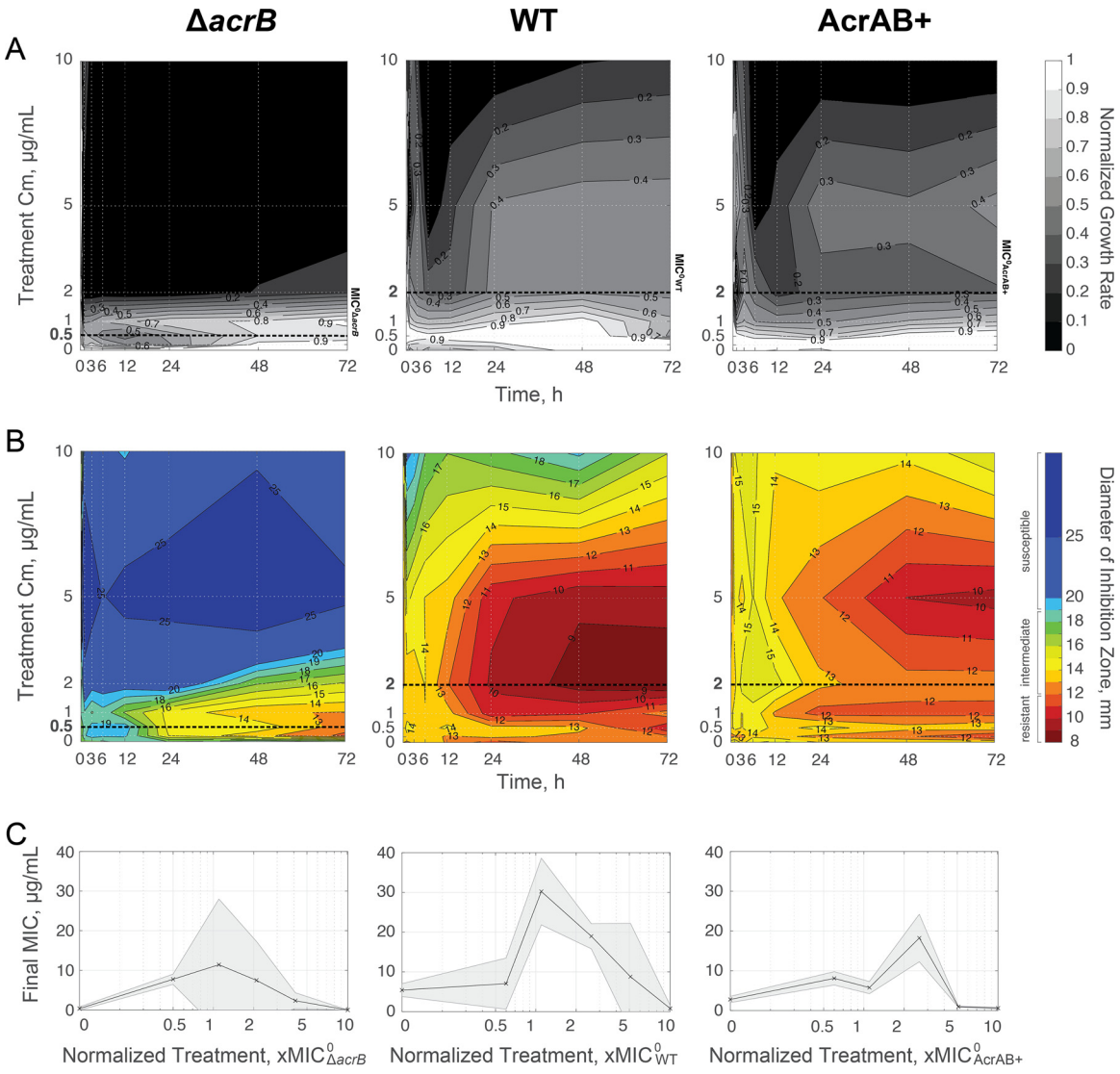

FIG 2 Temporal landscapes based on treatment concentration of chloramphenicol. (A) Average growth rate. Growth rates are normalized to growth of strains at $t = 0$ h; for raw data, see Fig. S1. Lighter areas represent growth rates closer to pretreatment values; darker areas represent reduced growth rates. MIC^0_{parent} is denoted with a bold dashed line for each strain (Fig. S2). (B) Average resistance. Diameter of inhibition zones were plotted for each time and treatment. Smaller inhibition zones are shown in red and correspond to resistant cells (≤12 mm), and larger inhibition zones are shown in blue and represent susceptible cells (≥19 mm); intermediate inhibition is shown with a color scale from orange to green. MIC^0_{parent} is denoted with a bold dashed line. (C) Final resistance at 72 h based on treatment concentration normalized to MIC^0_{parent}. The final, absolute MIC is calculated based on data from Fig. S5. Data points show the mean from three biological replicates. Shaded error bars show standard deviation.

treatment with high concentrations of chloramphenicol repressed bacterial growth for multiple days. We observed this growth inhibition at ~10 μg/ml for the WT and AcrAB$^+$ strains, and at ~2 μg/ml for the Δ*acrB* mutant. These inhibitory concentrations represent treatments of ~5× MIC^0_{parent} for all three strains. We found that cultures grown in lower chloramphenicol concentrations were able to recover growth. For example, when we treated cultures with ~1 to 2× MIC^0_{parent}, we observed a significant decrease in the growth rate between 0 and 12 h (see Table S1 in the supplemental material). However, after 12 to 24 h, growth in these populations was partially restored. At lower treatment concentrations (<1× MIC^0_{parent}), all cultures were able to grow, although usually at a deficit compared to the 0 μg/ml chloramphenicol condition. For all three strains, there were qualitatively similar growth recovery patterns, with an initial growth repression phase followed by a partially restored growth phase (Fig. S1).

The growth rate results suggested the evolution of drug resistance within the population (9, 18). To quantify this, we used an antibiotic disc assay to map the corresponding resistance levels (Fig. 2B; see Fig. S3 in the supplemental material). We found distinct increases in resistance levels that corresponded to populations that recovered growth. While there were qualitative similarities for the three strains, the timing and level of resistance achieved were dependent on the strain background. We classified populations as resistant when their inhibition zone diameters were smaller than 12 mm, following established standards for antimicrobial susceptibility testing (44). The WT strain gained resistance under a broad range of chloramphenicol treatment concentrations; this resistance emerged within 24 h when cells were treated with ~1 to 2× MIC^0_{WT}. The $AcrAB^+$ strain, where efflux pumps are overexpressed, was able to evolve resistance as well, albeit at a lower rate and at lower levels than the WT. The $AcrAB^+$ strain achieved resistance within 48 h when treated with 2.5× MIC^0_{AcrAB+}, but the range of chloramphenicol concentrations that resulted in resistance was narrower than for the WT strain. The Δ*acrB* cells achieved resistance more slowly, but for the range of ~1 to 2× $MIC^0_{\Delta acrB}$, cells in chloramphenicol cultures were still able to reach resistant levels (Fig. 2B; Fig. S3).

To compare the ultimate evolved resistance levels, we calculated the final, absolute MIC of the populations at 72 h. When we normalized the treatment concentration by MIC^0_{parent}, we found that treatments with concentrations of ~1 to 2× MIC^0_{parent} evolved the most resistant populations (Fig. 2C). Selective pressures of subinhibitory antibiotic concentrations have often been considered high risk for the evolution of resistance (14, 45). Yet, our results indicated that concentrations near or just above MIC^0_{parent} lead to the highest resistance levels under these conditions. In short, all three strains were able to evolve resistance when treated with ~1 to 2× MIC^0_{parent} of chloramphenicol, with the WT strain achieving the highest final, absolute MIC of the three strains. The WT evolved more rapidly than the $AcrAB^+$ or Δ*acrB* strain. Moreover, the relative range of chloramphenicol concentrations that supported the evolution of resistance in the $AcrAB^+$ strain was narrower than those for the WT or Δ*acrB* strains.

We next asked how resistance and growth changed through time. We found that in the absence of antibiotics, the trajectories trended largely toward faster growth, with minimal changes to resistance levels (Fig. 3). With subinhibitory chloramphenicol treatments, we observed that the populations first experienced a slight growth decrease, followed by increased resistance, and then showed restored growth within 48 h. While these populations did gain resistance, they did not tend to reach very high final MIC values in absolute terms, with inhibition zone diameters just at the border of being defined as resistant. In contrast, with inhibitory chloramphenicol treatment, there was a more dramatic reduction in growth within the first 12 h. Although growth was impacted, the populations tended to walk toward high resistance during this period. As depicted in the schematics, the zig-zag patterns trending toward high resistance may be indicative of the cultures acquiring resistant mutations and compensating for the associated fitness costs of these mutations. Finally, at high chloramphenicol concentrations, bacteria first became more susceptible and then stopped growing entirely within 12 h; growth was never restored for these populations. We found that all strains followed similar evolutionary trajectories while balancing the trade-off between growth and resistance. These findings highlight the importance of using antibiotic concentrations that are sufficiently inhibitory.

While these results tell us about the growth rate and resistance of the overall population, it is difficult to determine if subpopulations of cells within the culture have acquired high levels of resistance from disc assays alone. First, because the disc assays do not quantify resistance associated with individual cells in the culture, they cannot reveal the presence of subpopulations of resistant and susceptible cells. Second, beyond a certain resistance level, cells will grow up to the boundary of the disc; thus, it is not possible to quantify resistance increases beyond this. Determining which conditions can give rise to high levels of resistance is important

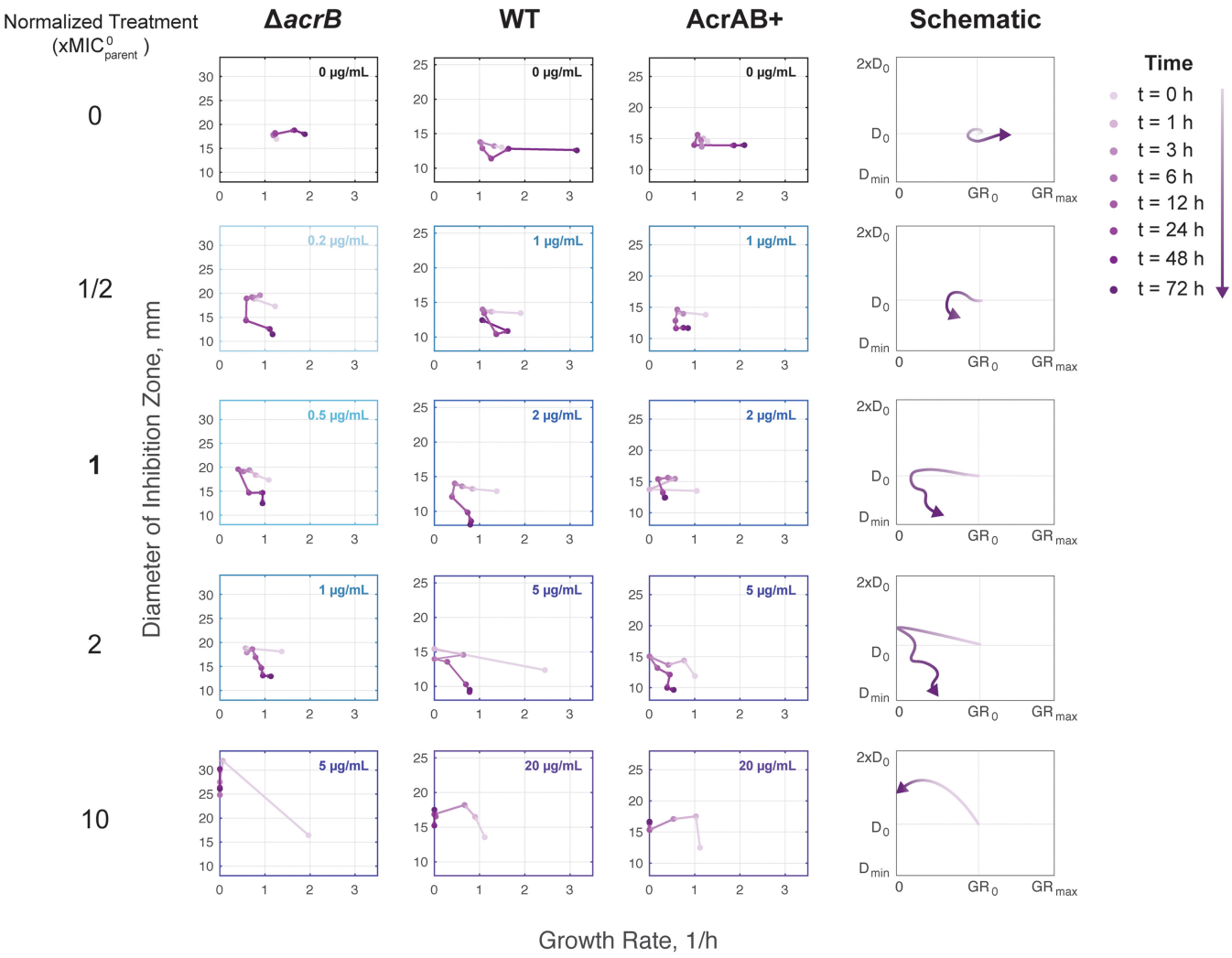

FIG 3 Resistance and fitness evolution trajectories. Average diameter of inhibition zone and average growth rate plotted against each other. Lighter purple markers represent trajectories occurring earlier; darker purple markers are later time points. The longer the distance between markers, the greater the change between time points. Colors of boxes indicate the absolute treatment concentration for the depicted trajectories. Schematics summarize patterns for each treatment concentration ($\times MIC^0_{parent}$). Schematic plots show growth rate in terms of initial growth rate (GR_0) and maximum physiological growth rate (GR_{max}). Resistance is shown in terms of relative diameter of inhibition, where D_0 is the diameter of inhibition at $t = 0$ h and D_{min} is the diameter of the antibiotic disc.

for revealing particularly dangerous treatment regimens. In addition, subpopulations with increased resistance to one antibiotic can promote cross-resistance to other drugs (45).

To quantify the fraction of resistant cells that emerged during our evolution experiment, we conducted a spot assay, in which we measured the fraction of the population capable of surviving on specific chloramphenicol concentrations. For all three strains, we observed subpopulations that were capable of growing on 10 μg/ml chloramphenicol (Fig. 4A; see Fig. S4 in the supplemental material). Interestingly, these cells primarily emerged from treatment conditions with lower levels of chloramphenicol, and not from conditions where cells were subjected to 10 μg/ml chloramphenicol. For example, at least 0.1% of the population from each of the three WT replicates that were treated with 2 μg/ml chloramphenicol could survive on 10 μg/ml at the end of the experiment. We did find cases where WT cells treated with 10 μg/ml evolved resistance to 10 μg/ml; however, this was less common than at lower treatment concentrations. Thus, cultures were able to evolve resistance to higher levels of chloramphenicol than they were subjected to, a feature that was most pronounced when treatments were just above or at MIC^0_{WT}. These results closely match trends in

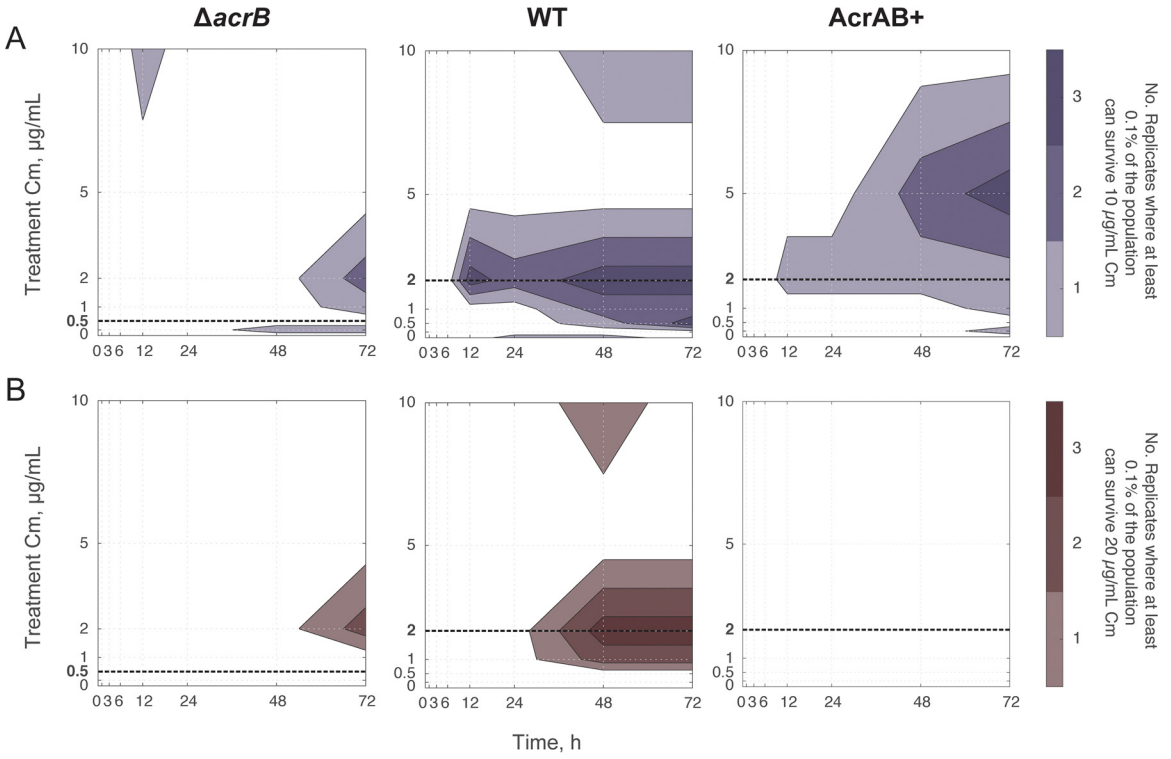

FIG 4 Number of biological replicates with highly resistant subpopulations through time. Shown are the numbers of biological replicates that had a subpopulation greater than 0.1% of their total population, which could grow on LB plates containing (A) 10 μg/ml or (B) 20 μg/ml chloramphenicol. Raw data are shown in Fig. S4. Initial populations contained ~10^7 CFU. MIC^0_{parent} is denoted with a bold dashed line.

the population's overall resistance (Fig. 2B). We also found isolates capable of growing on 20 μg/ml chloramphenicol, with a reduced frequency relative to 10 μg/ml (Fig. 4B; Fig. S4).

In contrast, the AcrAB$^+$ strain was capable of evolving resistance to 10 μg/ml when treated with 5 μg/ml chloramphenicol; yet, surprisingly, the AcrAB$^+$ strain never produced a subpopulation that was able to grow on 20 μg/ml as the WT did. Meanwhile, despite the higher initial susceptibility of the Δ*acrB* strain ($MIC^0_{\Delta acrB} < MIC^0_{WT}$ and MIC^0_{AcrAB+}), the Δ*acrB* strain consistently produced subpopulations that were able to grow at 20 μg/ml chloramphenicol by 72 h. This subpopulation appeared for chloramphenicol concentrations around 2 μg/ml, similar to the WT strain.

A key question remained: which mutations were responsible for the increases in resistance we observed? To address this, we used whole-genome sequencing to analyze three biological replicates from the 72-h time point for the WT, AcrAB$^+$, and Δ*acrB* strains (see Table S2 in the supplemental material). For the WT strain, each of the sequenced isolates contained a single point mutation in the DNA binding region of *marR*, which can upregulate AcrAB-TolC efflux pumps and expression of other stress response genes (46). Two of these point mutations were missense mutations in *marR* and have been observed in other studies (47–51). Additionally, one isolate had a missense mutation in the periplasmic encoding region of *acrB*. The other two isolates had an IS*1* or IS*5* insertional sequence interrupting *acrR*, which is known to upregulate *acrAB* (52). One question these results raise is why the AcrAB$^+$ strain, where *acrR* is removed, is outperformed by WT strains with mutations in *acrR*. A potential explanation for this is that the "marbox" through which *acrAB* is upregulated sits within *acrR* (53). The AcrAB$^+$ strain lacks this marbox (54), while in the sequenced isolates the insertion sequence is located further upstream in *acrR* and the marbox remains intact, providing global stress response regulation while eliminating the impact of the local

repressor. Thus, the exact position of the insertion sequence matters. These sequencing results indicate that strains containing AcrAB-TolC efflux pumps use mutations related to the pumps and their regulation to optimize survival and increase resistance in the presence of chloramphenicol.

When we evolved the AcrAB$^+$ strain and performed whole-genome sequencing of the most resistant isolates, all isolates had mutations in the noncoding, promoter region of *acrAB* (Table S2). These mutations indicate that the AcrAB$^+$ strain might require further tuning of *acrAB* expression for improved resistance. Furthermore, two of these isolates also had missense mutations in the coding region of *acrB* as well. Of these, the V139F missense mutation is known to produce high levels of multidrug resistance by accelerating export for a number of AcrAB-TolC substrates (11, 18, 55, 56). We observed *acrB* (Q569L) evolve from two different parent strains, the WT and AcrAB$^+$ strains, suggesting it plays a role in chloramphenicol export. Additionally, the evolved AcrAB$^+$ isolates all had other mutations less directly related to the AcrAB-TolC efflux pump and its regulators, such as genes related to transcription (*rpoB* and *yhjB*), fimbria assembly (*fimD*), or degradation (*clpX*) (Table S2).

In contrast, when we evolved the Δ*acrB* strain, we found that all three isolates had an insertion sequence located in *acrS* (Table S2). AcrS is the local regulator of the AcrEF-TolC efflux pump, a homolog to AcrAB-TolC (57). This result agrees with findings from Cudkowicz and Schuldiner, who showed that the Δ*acrB* strain gained high resistance by upregulating redundant efflux pumps in *E. coli*, such as AcrEF-TolC or MdtEF-TolC (11). One of the three isolates also contained a missense mutation in the selenocysteine synthase (*selA*) and a short insertion sequence in the 16S rRNA of the 30S subunit (*rrsG*), although whether or how these play a role in chloramphenicol resistance is unclear.

DISCUSSION

In this work, we identified that treatment of strains with antibiotic concentrations close to MIC^0_{parent} promotes the evolution of resistance; however, the evolvability and ultimate resistance level achieved differed between WT, AcrAB$^+$, and Δ*acrB* strains. WT populations evolved mutations that conferred high levels of resistance within 24 h after antibiotic exposure. Maximal resistance was evolved at ~1× MIC^0_{WT}; however, 0.25 to 2.5× MIC^0_{WT} chloramphenicol treatment concentrations all gave rise to resistance. In contrast, the AcrAB$^+$ strain evolved resistance, but this was only possible at precise chloramphenicol concentrations at 2.5× MIC^0_{AcrAB+}. The evolved AcrAB$^+$ populations were less resistant than their WT counterparts, and spot assays determining resistance confirmed this trend. In contrast, the Δ*acrB* strain was able to evolve resistance in 1 to 4× $MIC^0_{\Delta acrB}$ chloramphenicol treatments and ultimately achieved absolute resistance levels comparable to those observed in the WT strain.

Our results identify that antibiotic treatments near MIC^0_{parent} are especially prone to evolving resistance. Reding et al. observed this hot spot for adaptability of *E. coli* in the presence of another antibiotic, erythromycin, just below the MIC of their parent strains (20). While doctors measure resistance of bacterial infections, they sometimes prescribe antibiotic treatment prior to obtaining the results of this assay (58) or use a treatment concentration too low to effectively penetrate the infection site (59). This blind treatment could lead to increased levels of resistance (60, 61). These results highlight the presence of regimens that are especially problematic and which should be avoided to limit the evolution of antibiotic resistance.

While we observed that all strains were capable of evolving resistance, sequencing revealed the different pathways that each strain took to achieve this. The WT strain achieved resistance through mutations and insertion sequences in the regulators AcrR and MarR, suggesting that WT cells can fine-tune expression of the AcrAB-TolC pumps to gain resistance to chloramphenicol. Interestingly, these mutations may produce cross-resistance to other antibiotics as well since these regulators control many genes involved in multidrug resistance (62, 63). AcrAB$^+$ cells utilized mutations in *acrB* and the promoter region

controlling its expression to achieve resistance. Δ*acrB* populations achieved resistance by targeting homologous efflux pump systems, such as AcrEF-TolC. Although resistance was slow to emerge in this strain compared to the WT or AcrAB$^+$ strain, this alternative pathway for achieving resistance ultimately resulted in levels comparable to those achieved by the WT strain. By charting evolutionary landscapes across different antibiotic concentrations, we have gained insight into treatments that impact the emergence of antibiotic resistance and the effect of efflux pumps on this process.

MATERIALS AND METHODS

Bacterial strains. We used *E. coli* strains BW25113 (WT), BW25113 Δ*acrR* (AcrAB$^+$), and BW25113 Δ*acrB* (Δ*acrB*) as the parent strains. The WT strain BW25113 is the base strain for the Keio collection (54). For BW25113 Δ*acrR*, we designed primers with homology regions on *acrR* and amplified the kanamycin resistance marker and FRT (FLP recombination target) sites of pKD13 (54). Primers are listed in Table S3 in the supplemental material. The linear DNA was then treated using a DpnI digest and PCR purification. We electroporated the purified linear DNA into competent BW25113 cells containing the plasmid pSIM6 (64). BW25113 Δ*acrB* was derived from Keio collection strain JW0451 (BW25113 Δ*acrB*::Kan^r) (26). We removed kanamycin resistance markers from BW25113 Δ*acrR*::Kan^r and JW0451 following the pCP20 protocol from reference 65.

Determination of MIC. For all experiments, overnight cultures were inoculated from a single colony in 10 ml LB and grown in a 50-ml Erlenmeyer flask at 37°C with 200-rpm orbital shaking. After overnight growth, the optical density at 600 nm (OD_{600}) was measured, and the initial volume was diluted back to OD_{600} = 0.1. To determine the MICs of the parent strains (Fig. S2), we added a final concentration of 0, 0.2, 0.5, 1, 2, 4, 8, or 12 μg/ml chloramphenicol to each culture. To determine the MICs of the evolved strains (see Fig. S5 in the supplemental material), we added 0, 0.5, 1, 2, 5, 10, 20, or 50 μg/ml to each culture. Chloramphenicol stocks were prepared with 100% ethanol. The samples were sealed with evaporation-limiting membranes (Thermo Scientific AB-0580) and grown in 24-well plates at 37°C with 200-rpm orbital shaking. OD_{600} readings were taken using a BioTek Synergy H1m plate reader before incubation (t = 0 h) and after antibiotic exposure (t = 24 h). All experiments were performed in triplicate using biological replicates.

Experimental conditions in the eVOLVER. In the eVOLVER, cultures were inoculated from a single colony in LB at 37°C. A stir bar mixed the cultures on a medium setting, or approximately 1,000 rpm (39). The LB was supplemented with the detergent Tween 20 (Sigma-Aldrich catalog no. P1379) at 0.2% (vol/vol) to reduce spurious OD_{600} measurements caused by biofilm growth on the flask. As Tween 20 is a detergent and a potential substrate of the AcrAB-TolC efflux pumps, we also conducted the toxicity curve experiments with Tween 20 at our working concentration of 0.2% (vol/vol). We found there was no significant change in resistance for any of the strains in the presence of Tween 20 (see Fig. S6 and Table S4 in the supplemental material).

Cells were inoculated in the eVOLVER overnight ($t \approx -16$ to -14 h) prior to the beginning of the experiment (t = 0 h) to establish steady-state exponential growth. We set the eVOLVER using an upper OD_{600} bound of 0.2 and a lower bound of 0.1; thus, cultures were grown to a turbidity of 0.2 and then diluted back to 0.1 to maintain the turbidostat at an approximately constant cell density. Samples were collected during the experiment at set time points (t = 0, 1, 3, 6, 12, 24, 48, and 72 h) and used for downstream analysis. All experiments were performed in triplicate using biological replicates.

At t = 0 h, we introduced chloramphenicol at a predetermined final treatment concentration (0, 0.2, 0.5, 1, 2, 5, 10, or 20 μg/ml). This introduction was implemented by switching the source of the medium from one containing 0 μg/ml chloramphenicol to another containing the final treatment concentration; in addition, we spiked the samples directly with the treatment concentration of chloramphenicol at the same time to avoid a delay due to the time required for cycling of the medium in the turbidostat.

Downstream assays and data collection from eVOLVER samples. (i) Growth rate measurements. Growth rate measurements were calculated after each dilution event using the following equation:

$$\text{Growth rate} = \frac{\ln\left(\frac{OD_{600,\,high}}{OD_{600,\,low}}\right)}{t_{OD_{600,\,high}} - t_{OD_{600,\,low}}}$$

The growth rate between each dilution was then averaged across sampling time points to compare against disc diffusion assays and spot assays. For example, the growth rate given at t = 0 h is the growth rate from $t = -6$ h to t = 0 h. To evaluate statistically significant differences in growth rate between two time points, we used the paired t test; to evaluate statistically significant differences in growth rate between two strains, we used the t test (Table S1A).

(ii) Antibiotic disc diffusion assay. We aliquoted samples from the eVOLVER, where the OD_{600} from each sample was between 0.1 and 0.2. We used cotton swabs to cover LB agar plates with a layer of the sample (66). An antibiotic disc containing chloramphenicol (30 g) (Thermo Fisher Scientific catalog no. CT0013B) was then placed on the plate. The plate was incubated for 24 h at 37°C. The diameter of the zone of inhibition around each disc was then measured. Diameters of inhibition zones were classified as susceptible, intermediate, or resistant based on reference 44. Additionally, we calculated the MIC using a mapping between the MIC and the diameter of inhibition zone for our samples (Fig. S5) (67). To evaluate statistically significant differences in diameter of inhibition zones or resistance between two time points,

we used the paired *t* test; to evaluate statistically significant differences in resistance between two genotypes, we used the *t* test (Table S1B).

(iii) Spot assay. The samples from the eVOLVER experiment were diluted in phosphate-buffered saline (PBS) in the following dilution series: 1, 10^{-1}, 10^{-2}, 10^{-3}, 10^{-4}, and 10^{-5}. We then plated 2.5 μl of each dilution on LB agar plates containing 0, 0.5, 1, 2, 5, 10, and 20 μg/ml chloramphenicol. The plates were then incubated for 24 h at 37°C. To count colonies, we identified the dilution factor with the most countable colonies and recorded the number of CFU and dilution factor (*d*). The number of CFU/ml for each sample was then calculated as CFU/ml = (CFU $\times$ *d*)/*V*, where *V* is the volume plated. We also calculated the proportion of the population able to grow on different concentrations of chloramphenicol by calculating the CFU/ml from LB agar plates containing 0, 0.5, 1, 2, 5, 10, and 20 μg/ml chloramphenicol.

Whole-genome sequencing. DNA was extracted from single isolates and parent strains using the Qiagen DNeasy PowerBiofilm kit. For each strain, we selected three isolates to sequence; each of these isolates originated from a different biological replicate that was evolved under the same experimental conditions (i.e., each isolate comes from a different eVOLVER culture). Samples were sequenced at the Microbial Genome Sequencing Center (MiGS) in Pittsburg, PA, USA, who conducted library preparation and multiplexing using the Illumina Nextera kit series and then sequenced using a NextSeq 550 platform with 150-bp paired ends and an average coverage of 50 reads. We analyzed reads using version 0.35.1 of *breseq* (68). Reads were aligned to the BW25113 Keio reference genome (accession no. CP009273) in consensus mode. The treatment concentrations and isolation concentrations used to select each isolate are listed in Table S2.

Data availability. Whole-genome sequencing data for the parent strains and the isolates are available in GenBank under BioProject no. PRJNA666010 and accession no. CP062239 to CP062250. Other data sets generated during this study are available from the corresponding author upon request.

SUPPLEMENTAL MATERIAL

Supplemental material is available online only.

FIG S1, TIF file, 1.8 MB.

FIG S2, TIF file, 0.1 MB.

FIG S3, TIF file, 1.9 MB.

FIG S4, TIF file, 2.1 MB.

FIG S5, TIF file, 0.5 MB.

FIG S6, TIF file, 2.9 MB.

TABLE S1, XLSX file, 0.02 MB.

TABLE S2, DOCX file, 0.02 MB.

TABLE S3, DOCX file, 0.01 MB.

TABLE S4, DOCX file, 0.01 MB.

ACKNOWLEDGMENTS

This research was supported by the National Science Foundation (grant no. 1347635) and the National Institutes of Health (grant no. R01AI102922).

We thank Mo Khalil, Brandon Wong, Chris Mancuso, and Zack Heins for assistance and support with the eVOLVER.

REFERENCES

1. Smith PA, Koehler MFT, Girgis HS, Yan D, Chen Y, Chen Y, Crawford JJ, Durk MR, Higuchi RI, Kang J, Murray J, Paraselli P, Park S, Phung W, Quinn JG, Roberts TC, Rougé L, Schwarz JB, Skippington E, Wai J, Xu M, Yu Z, Zhang H, Tan MW, Heise CE. 2018. Optimized arylomycins are a new class of Gram-negative antibiotics. Nature 561:189–194. https://doi.org/10.1038/s41586-018-0483-6.
2. Sousa MC. 2019. New antibiotics target the outer membrane of bacteria. Nature 576:389–390. https://doi.org/10.1038/d41586-019-03730-x.
3. Imai Y, Meyer KJ, Iinishi A, Favre-Godal Q, Green R, Manuse S, Caboni M, Mori M, Niles S, Ghiglieri M, Honrao C, Ma X, Guo JJ, Makriyannis A, Linares-Otoya L, Böhringer N, Wuisan ZG, Kaur H, Wu R, Mateus A, Typas A, Savitski MM, Espinoza JL, O'Rourke A, Nelson KE, Hiller S, Noinaj N, Schäberle TF, D'Onofrio A, Lewis K. 2019. A new antibiotic selectively kills Gram-negative pathogens. Nature 576:459–464. https://doi.org/10.1038/s41586-019-1791-1.
4. Hart EM, Mitchell AM, Konovalova A, Grabowicz M, Sheng J, Han X, Rodriguez-Rivera FP, Schwaid AG, Malinverni JC, Balibar CJ, Bodea S, Si Q, Wang H, Homsher MF, Painter RE, Ogawa AK, Sutterlin H, Roemer T, Black TA, Rothman DM, Walker SS, Silhavy TJ. 2019. A small-molecule inhibitor of BamA impervious to efflux and the outer membrane permeability barrier. Proc Natl Acad Sci U S A 116:21748–21757. https://doi.org/10.1073/pnas.1912345116.
5. Luther A, Urfer M, Zahn M, Müller M, Wang SY, Mondal M, Vitale A, Hartmann JB, Sharpe T, Lo Monte F, Kocherla H, Cline E, Pessi G, Rath P, Modaresi SM, Chiquet P, Stiegeler S, Verbree C, Remus T, Schmitt M, Kolopp C, Westwood MA, Desjonquères N, Brabet E, Hell S, LePoupon K, Vermeulen A, Jaisson R, Rithié V, Upert G, Lederer A, Zbinden P, Wach A, Moehle K, Zerbe K, Locher HH, Bernardini F, Dale GE, Eberl L, Wollscheid B, Hiller S, Robinson JA, Obrecht D. 2019. Chimeric peptidomimetic antibiotics against Gram-negative bacteria. Nature 576:452–458. https://doi.org/10.1038/s41586-019-1665-6.
6. Davies J, Davies D. 2010. Origins and evolution of antibiotic resistance. Microbiol Mol Biol Rev 74:417–433. https://doi.org/10.1128/MMBR.00016-10.
7. Newton J, Fenton K. 2015. Health matters—tackling antimicrobial resistance. Public Health Matters. https://publichealthmatters.blog.gov.uk/2015/12/10/health-matters-tackling-antimicrobial-resistance/#:~:text=Health%20Matters%20%E2%80%93%20tackling%20antimicrobial%20resistance.%20Welcome%20to,and%20the%20Q%26A%20featuring%20questions%20submitted%20by%20.
8. Ventola CL. 2015. The antibiotic resistance crisis: part 1: causes and threats. Pharm Ther 40:277–283.

9. Toprak E, Veres A, Yildiz S, Pedraza JM, Chait R, Paulsson J, Kishony R. 2013. Building a morbidostat: an automated continuous-culture device for studying bacterial drug resistance under dynamically sustained drug inhibition. Nat Protoc 8:555–567. https://doi.org/10.1038/nprot.nprot.2013.021.
10. Toprak E, Veres A, Michel J-B, Chait R, Hartl DL, Kishony R. 2011. Evolutionary paths to antibiotic resistance under dynamically sustained drug selection. Nat Genet 44:101–105. https://doi.org/10.1038/ng.1034.
11. Alon Cudkowicz N, Schuldiner S. 2019. Deletion of the major *Escherichia coli* multidrug transporter AcrB reveals transporter plasticity and redundancy in bacterial cells. PLoS One 14:e0218828. https://doi.org/10.1371/journal.pone.0218828.
12. Yoshida M, Reyes SG, Tsuda S, Horinouchi T, Furusawa C, Cronin L. 2017. Time-programmable drug dosing allows the manipulation, suppression and reversal of antibiotic drug resistance *in vitro*. Nat Commun 8:15589. https://doi.org/10.1038/ncomms15589.
13. Marchant J. 2018. When antibiotics turn toxic. Nature 555:431–433. https://doi.org/10.1038/d41586-018-03267-5.
14. Wistrand-Yuen E, Knopp M, Hjort K, Koskiniemi S, Berg OG, Andersson DI. 2018. Evolution of high-level resistance during low-level antibiotic exposure. Nat Commun 9:1599. https://doi.org/10.1038/s41467-018-04059-1.
15. Kohanski MA, DePristo MA, Collins JJ. 2010. Sublethal antibiotic treatment leads to multidrug resistance via radical-induced mutagenesis. Mol Cell 37:311–320. https://doi.org/10.1016/j.molcel.2010.01.003.
16. Andersson DI, Hughes D. 2012. Evolution of antibiotic resistance at non-lethal drug concentrations. Drug Resist Updat 15:162–172. https://doi.org/10.1016/j.drup.2012.03.005.
17. Kaminski Strauss S, Schirman D, Jona G, Brooks AN, Kunjapur AM, Nguyen Ba AN, Flint A, Solt A, Mershin A, Dixit A, Yona AH, Csörgő B, Busby BP, Hennig BP, Pál C, Schraivogel D, Schultz D, Wernick DG, Agashe D, Levi D, Zabezhinsky D, Russ D, Sass E, Tamar E, Herz E, Levy ED, Church GM, Yelin I, Nachman I, Gerst JE, Georgeson JM, Adamala KP, Steinmetz LM, Rübsam M, Ralser M, Klutstein M, Desai MM, Walunjkar N, Yin N, Aharon Hefetz N, Jakimo N, Snitser O, Adini O, Kumar P, Soo Hoo Smith R, Zeidan R, Hazan R, Rak R, Kishony R, Johnson S, et alet al. 2019. Evolthon: a community endeavor to evolve lab evolution. PLoS Biol 17:e3000182. https://doi.org/10.1371/journal.pbio.3000182.
18. Jahn LJ, Munck C, Ellabaan MMH, Sommer MOA. 2017. Adaptive laboratory evolution of antibiotic resistance using different selection regimes lead to similar phenotypes and genotypes. Front Microbiol 8:816. https://doi.org/10.3389/fmicb.2017.00816.
19. Russ D, Glaser F, Shaer Tamar E, Yelin I, Baym M, Kelsic ED, Zampaloni C, Haldimann A, Kishony R. 2020. Escape mutations circumvent a tradeoff between resistance to a beta-lactam and resistance to a beta-lactamase inhibitor. Nat Commun 11. https://doi.org/10.1038/s41467-020-15666-2.
20. Reding C, Catalán P, Jansen G, Bergmiller T, Rosenstiel P, Schulenburg H, Gudelj I, Beardmore R. 2019. Hotspot dosages of most rapid antibiotic resistance evolution. bioRxiv 866269. https://www.biorxiv.org/content/10.1101/866269v1.
21. Delcour AH. 2009. Outer membrane permeability and antibiotic resistance. Biochim Biophys Acta 1794:808–816. https://doi.org/10.1016/j.bbapap.2008.11.005.
22. Blair JMA, Webber MA, Baylay AJ, Ogbolu DO, Piddock LV. 2015. Molecular mechanisms of antibiotic resistance. Nat Rev Microbiol 13:42–51. https://doi.org/10.1038/nrmicro3380.
23. Li X-Z, Plésiat P, Nikaido H. 2015. The challenge of efflux-mediated antibiotic resistance in Gram-negative bacteria. Clin Microbiol Rev 28:337–418. https://doi.org/10.1128/CMR.00117-14.
24. Kobylka J, Kuth MS, Müller RT, Geertsma ER, Pos KM. 2020. AcrB: a mean, keen, drug efflux machine. Ann N Y Acad Sci 1459:38–68. https://doi.org/10.1111/nyas.14239.
25. Nikaido H, Takatsuka Y. 2009. Mechanisms of RND multidrug efflux pumps. Biochim Biophys Acta 1794:769–781. https://doi.org/10.1016/j.bbapap.2008.10.004.
26. Langevin AM, Dunlop MJ. 2017. Stress introduction rate alters the benefit of AcrAB-TolC efflux pumps. J Bacteriol 200:e00525-17. https://doi.org/10.1128/JB.00525-17.
27. Okusu H, Ma D, Nikaido H. 1996. AcrAB efflux pump plays a major role in the antibiotic resistance phenotype of *Escherichia coli* multiple-antibiotic-resistance (Mar) mutants. J Bacteriol 178:306–308. https://doi.org/10.1128/jb.178.1.306-308.1996.
28. Zwama M, Yamasaki S, Nakashima R, Sakurai K, Nishino K, Yamaguchi A. 2018. Multiple entry pathways within the efflux transporter AcrB contribute to multidrug recognition. Nat Commun 9. https://doi.org/10.1038/s41467-017-02493-1.
29. Webber MA, Talukder A, Piddock LJV. 2005. Contribution of mutation at amino acid 45 of AcrR to *acrB* expression and ciprofloxacin resistance in clinical and veterinary *Escherichia coli* isolates. Antimicrob Agents Chemother 49:4390–4392. https://doi.org/10.1128/AAC.49.10.4390-4392.2005.
30. Olliver A, Vallé M, Chaslus-Dancla E, Cloeckaert A. 2004. Role of an *acrR* mutation in multidrug resistance of *in vitro*-selected fluoroquinolone-resistant mutants of *Salmonella enterica* serovar Typhimurium. FEMS Microbiol Lett 238:267–272. https://doi.org/10.1016/j.femsle.2004.07.046.
31. Wang H, Dzink-Fox JL, Chen M, Levy SB. 2001. Genetic characterization of highly fluoroquinolone-resistant clinical *Escherichia coli* strains from China: role of *acrR* mutations. Antimicrob Agents Chemother 45:1515–1521. https://doi.org/10.1128/AAC.45.5.1515-1521.2001.
32. Baym M, Lieberman TD, Kelsic ED, Chait R, Gross R, Yelin I, Kishony R. 2016. Spatiotemporal microbial evolution on antibiotic landscapes. Science 353:1147–1151. https://doi.org/10.1126/science.aag0822.
33. Singh R, Swick MC, Ledesma KR, Yang Z, Hu M, Zechiedrich L, Tam VH. 2012. Temporal interplay between efflux pumps and target mutations in development of antibiotic resistance in Escherichia coli. Antimicrob Agents Chemother 56:1680–1685. https://doi.org/10.1128/AAC.05693-11.
34. El Meouche I, Dunlop MJ. 2018. Heterogeneity in efflux pump expression predisposes antibiotic-resistant cells to mutation. Science 362:686–690. https://doi.org/10.1126/science.aar7981.
35. Lukačišinová M, Fernando B, Bollenbach T. 2020. Highly parallel lab evolution reveals that epistasis can curb the evolution of antibiotic resistance. Nat Commun 11:3105. https://doi.org/10.1038/s41467-020-16932-z.
36. Papkou A, Hedge J, Kapel N, Young B, MacLean RC. 2020. Efflux pump activity potentiates the evolution of antibiotic resistance across S. aureus isolates. Nat Commun 11. https://doi.org/10.1038/s41467-020-17735-y.
37. Sood S. 2016. Chloramphenicol—a potent armament against multi-drug resistant (MDR) Gram negative bacilli? J Clin Diagn Res 10:DC01–DC03. https://doi.org/10.7860/JCDR/2016/14989.7167.
38. Nitzan O, Kennes Y, Colodner R, Saliba W, EdelsteinI H, Raz R, Chazan B. 2015. Chloramphenicol use and susceptibility patterns in Israel: a national survey. Isr Med Assoc J 17:27–31.
39. Wong BG, Mancuso CP, Kiriakov S, Bashor CJ, Khalil AS. 2018. Precise, automated control of conditions for high-throughput growth of yeast and bacteria with eVOLVER. Nat Biotechnol 36:614–623. https://doi.org/10.1038/nbt.4151.
40. Ruiz C, Levy SB. 2014. Regulation of *acrAB* expression by cellular metabolites in *Escherichia coli*. J Antimicrob Chemother 69:390–399. https://doi.org/10.1093/jac/dkt352.
41. Luhe AL, Gerken H, Tan L, Wu J, Zhao H. 2012. Alcohol tolerance of Escherichia coli acrR and marR regulatory mutants. J Mol Catal B Enzym 76:89–93. https://doi.org/10.1016/j.molcatb.2011.11.013.
42. Subhadra B, Kim J, Kim DH, Woo K, Oh MH, Choi CH. 2018. Local repressor AcrR regulates AcrAB efflux pump required for biofilm formation and virulence in Acinetobacter nosocomialis. Front Cell Infect Microbiol 8:270. https://doi.org/10.3389/fcimb.2018.00270.
43. Chetri S, Bhowmik D, Paul D, Pandey P, Chanda DD, Chakravarty A, Bora D, Bhattacharjee A. 2019. AcrAB-TolC efflux pump system plays a role in carbapenem non-susceptibility in Escherichia coli. BMC Microbiol 19:210. https://doi.org/10.1186/s12866-019-1589-1.
44. Clinical and Laboratory Standards Institute. 2013. M100-S23 performance standards for antimicrobial susceptibility testing; twenty-third informational supplement, 33rd ed. Clinical and Laboratory Standards Institute, Wayne, PA.
45. Andersson DI, Balaban NQ, Baquero F, Courvalin P, Glaser P, Gophna U, Kishony R, Molin S, Tønjum T. 2020. Antibiotic resistance: turning evolutionary principles into clinical reality. FEMS Microbiol Rev 44. https://doi.org/10.1093/femsre/fuaa001.
46. McMurry LM, Levy SB. 2013. Amino acid residues involved in inactivation of the *Escherichia coli* multidrug resistance repressor MarR by salicylate, 2,4-dinitrophenol, and plumbagin. FEMS Microbiol Lett 349:16–24. https://doi.org/10.1111/1574-6968.12291.
47. Linkevicius M, Sandegren L, Andersson DI. 2013. Mechanisms and fitness costs of tigecycline resistance in Escherichia coli. J Antimicrob Chemother 68:2809–2819. https://doi.org/10.1093/jac/dkt263.
48. Lu J, Jin M, Nguyen SH, Mao L, Li J, Coin LJM, Yuan Z, Guo J. 2018. Non-antibiotic antimicrobial triclosan induces multiple antibiotic resistance through genetic mutation. Environ Int 118:257–265. https://doi.org/10.1016/j.envint.2018.06.004.
49. Ching C, Zaman MH. 2020. Development and selection of low-level multidrug resistance over an extended range of sub-inhibitory ciprofloxacin

concentrations in Escherichia coli. Sci Rep 10:8754. https://doi.org/10.1038/s41598-020-65602-z.
50. Lázár V, Kishony R. 2019. Transient antibiotic resistance calls for attention. Nat Microbiol 4:1606–1607. https://doi.org/10.1038/s41564-019-0571-x.
51. Hickman RA, Munck C, Sommer MOA. 2017. Time-resolved tracking of mutations reveals diverse allele dynamics during Escherichia coli antimicrobial adaptive evolution to single drugs and drug pairs. Front Microbiol 8:893. https://doi.org/10.3389/fmicb.2017.00893.
52. Grenier F, Matteau D, Baby V, Rodrigue S. 2014. Complete genome sequence of *Escherichia coli* BW25113. Genome Announc 2:e01038-14. https://doi.org/10.1128/genomeA.01038-14.
53. Watanabe R, Doukyu N. 2012. Contributions of mutations in acrR and marR genes to organic solvent tolerance in Escherichia coli. AMB Express 2:58. https://doi.org/10.1186/2191-0855-2-58.
54. Baba T, Ara T, Hasegawa M, Takai Y, Okumura Y, Baba M, Datsenko KA, Tomita M, Wanner BL, Mori H. 2006. Construction of *Escherichia coli* K-12 in-frame, single-gene knockout mutants: the Keio collection. Mol Syst Biol 2:2006.0008. https://doi.org/10.1038/msb4100050.
55. Kinana AD, Vargiu AV, Nikaido H. 2013. Some ligands enhance the efflux of other ligands by the Escherichia coli multidrug pump AcrB. Biochemistry 52:8342–8351. https://doi.org/10.1021/bi401303v.
56. Hoeksema M, Jonker MJ, Brul S, Ter Kuile BH. 2019. Effects of a previously selected antibiotic resistance on mutations acquired during development of a second resistance in Escherichia coli. BMC Genomics 20:284. https://doi.org/10.1186/s12864-019-5648-7.
57. Hirakawa H, Takumi-Kobayashi A, Theisen U, Hirata T, Nishino K, Yamaguchi A. 2008. AcrS/EnvR represses expression of the acrAB multidrug efflux genes in Escherichia coli. J Bacteriol 190:6276–6279. https://doi.org/10.1128/JB.00190-08.
58. Ray MJ, Tallman GB, Bearden DT, Elman MR, McGregor JC. 2019. Antibiotic prescribing without documented indication in ambulatory care clinics: national cross sectional study. BMJ 367:l6461. https://doi.org/10.1136/bmj.l6461.
59. Falagas ME, Makris GC, Dimopoulos G, Matthaiou DK. 2008. Heteroresistance: a concern of increasing clinical significance? Clin Microbiol Infect 14:101–104. https://doi.org/10.1111/j.1469-0691.2007.01912.x.
60. Hennessy TW, Petersen KM, Bruden D, Parkinson AJ, Hurlburt D, Getty M, Schwartz B, Butler JC. 2002. Changes in antibiotic-prescribing practices and carriage of penicillin-resistant *Streptococcus pneumoniae*: a controlled intervention trial in rural Alaska. Clin Infect Dis 34:1543–1550. https://doi.org/10.1086/340534.
61. Čižman M. 2003. The use and resistance to antibiotics in the community. Int J Antimicrob Agents 21:297–307. https://doi.org/10.1016/S0924-8579(02)00394-1.
62. Barbosa TM, Levy SB. 2000. Differential expression of over 60 chromosomal genes in Escherichia coli by constitutive expression of MarA. J Bacteriol 182:3467–3474. https://doi.org/10.1128/jb.182.12.3467-3474.2000.
63. Alekshun MN, Levy SB. 1999. The mar regulon: multiple resistance to antibiotics and other toxic chemicals. Trends Microbiol 7:410–413.
64. Datta S, Costantino N, Court DL. 2006. A set of recombineering plasmids for Gram-negative bacteria. Gene 379:109–115. https://doi.org/10.1016/j.gene.2006.04.018.
65. Datsenko KA, Wanner BL. 2000. One-step inactivation of chromosomal genes in *Escherichia coli* K-12 using PCR products. Proc Natl Acad Sci U S A 97:6640–6645. https://doi.org/10.1073/pnas.120163297.
66. Andrews JM, BSAC Working Party on Susceptibility Testing. 2001. BSAC standardized disc susceptibility testing method. J Antimicrob Chemother 48:43–57. https://doi.org/10.1093/jac/48.suppl_1.43.
67. Kronvall G. 1982. Analysis of a single reference strain for determination of gentamicin regression line constants and inhibition zone diameter breakpoints in quality control of disk diffusion antibiotic susceptibility testing. J Clin Microbiol 16:784–793. https://doi.org/10.1128/JCM.16.5.784-793.1982.
68. Deatherage DE, Barrick JE. 2014. Identification of mutations in laboratory-evolved microbes from next-generation sequencing data using breseq. Methods Mol Biol 1151:165–188. https://doi.org/10.1007/978-1-4939-0554-6_12.